BBC RD 1973/13

BBC

1969
THE QUEEN'S AWARD
TO INDUSTRY

RESEARCH DEPARTMENT

REPORT

# M.F. PROPAGATION: a wave-hop method for ionospheric field-strength prediction

P. Knight, M.A., Ph.D., M.I.E.E.

Research Department, Engineering Division
THE BRITISH BROADCASTING CORPORATION August 1973 (RA-113)

BBC RD 1973/13
UDC 621.391.812.8

# MF PROPAGATION: A WAVE-HOP METHOD FOR IONOSPHERIC FIELD-STRENGTH PREDICTION

P. Knight, M.A., Ph.D., M.I.E.E.

## Summary

*A new method for calculating the strength of medium-frequency sky-wave signals at night is described. Estimated losses due to all the ionospheric and terrestrial factors which affect a wave as it propagates from transmitter to receiver are subtracted from the field strength which would arise if losses were absent. This process is carried out for each propagation mode which is likely to make a significant contribution to the received signal; the contributions are then added on a power basis. The method is intended for world-wide application and for paths of any length. Field strengths predicted by this method for 152 paths in different parts of the world have been found to agree reasonably well with measured values.*

Issued under the authority of

P. Laurie

Head of Research Department

Research Department, Engineering Division,
BRITISH BROADCASTING CORPORATION

(RA-113)

# MF PROPAGATION: A WAVE-HOP METHOD FOR IONOSPHERIC FIELD-STRENGTH PREDICTION

August 1973

BBC RD 1973/13
UDC 621.391.812.8

# MF PROPAGATION: A WAVE-HOP METHOD FOR IONOSPHERIC FIELD-STRENGTH PREDICTION

P. Knight, M.A., Ph.D., M.I.E.E.

## 1. Introduction

This report describes a new method for predicting night-time sky-wave field strengths at medium frequencies, which is intended for world-wide application and for paths of any length. It is called the wave-hop method because of its similarity to the wave-hop propagation theory for v.l.f. described by the CCIR.[1]

In its present form the method calls for an appreciable number of charts and curves, described in the sections which follow, and a certain amount of engineering judgement. It should, however, be possible to adapt it to a computer; some parts of the calculation would, in fact, be more conveniently performed with a computer because of the large number of variables involved. It may also be possible to achieve a worth-while simplification by using the charts and curves to calculate propagation curves for typical conditions, with correction curves for less-typical conditions.

The method is described in detail in Section 2 and an example of its application given in Section 3. Section 4 gives results of comparisons between predicted and measured field strengths.

## 2. The wave-hop method

In the wave-hop method, median field strengths are calculated individually for each ionospheric mode which is likely to contribute significantly to the field strength at the receiver. The calculation takes into account all the ionospheric and terrestrial factors which affect the wave as it propagates from transmitter to receiver. In applying the method, the first step is to use charts to determine which ionospheric modes are likely to be important. For each mode which needs to be considered, convergence gains is added to the unattenuated field strength and the following losses subtracted:

Ground loss at transmitter and receiver

Polarisation coupling loss at transmitter and receiver

Ionospheric loss

Intermediate reflection loss (for multi-hop modes)

A transmitting aerial correction is then applied to each of the modes and, if two or more are of comparable strength, their powers are added.

The calculation gives the median field strength which should be observed after sunset when nocturnal conditions are well established over the entire path. The predicted field strength also corresponds to minimum solar activity. Further corrections may then be applied to determine the quasi-maximum field strength, or the field-strength at times nearer sunset or sunrise, or at some other point in the solar cycle.

### 2.1. Mode selection

Although m.f. propagation is mainly via the E-layer, F-layer reflections may occur at short distances at the higher frequencies in the band. Fig. 1(*a*) shows the reflections which are likely to occur six hours after sunset if the critical frequency varies in the manner described in Reference 2. It also shows that E- and F-layer reflections may be received simultaneously on short-distance paths.

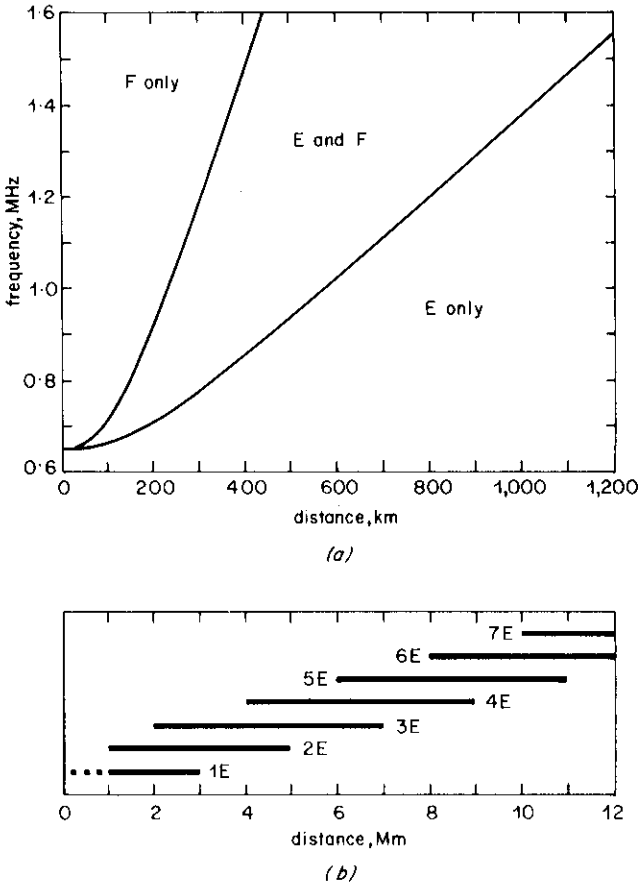


*Fig. 1 - Mode selection charts*

(*a*) One-hop modes propagating six hours after sunset

(*b*) E-layer modes propagating to longer distances

At distances greater than 1200 km, single-hop modes are unable to penetrate the E-layer, and multi-hop F-layer reflections do not usually contribute significantly to the received signal. At the longer distances, therefore, E-layer reflections are the only propagation modes which need to be considered and Fig. 1(*b*) shows the modes which should be taken into consideration. Fig. 1(*b*) takes account of diffraction around the curvature of the Earth; this may considerably extend the effective range of low-angle modes, especially when one of the terminals is situated close to the sea.

### 2.2. Unattenuated field-strength

The basic field strength to which convergence gain is added and from which all other losses subtracted, is shown in Fig. 2. This is the field strength which would be measured if the transmitter radiated with a cymomotive force (c.m.f.) of 300 volts in all directions above the horizontal and if the Earth and ionosphere behaved as perfect plane reflectors. The receiver is assumed to be connected to a loop or ferrite-rod aerial near the ground with its axis perpendicular to the direction of the transmitter; this orientation normally gives maximum pick-up.* With these assumptions, the unattenuated field-strength is given by

$$E = 66 + 20 \log_{10} \frac{300}{d} \qquad (1)$$

where $E$ is in dBs relative to 1 $\mu$V/m and $d$ is the path length via the ionosphere. Equation (1) includes 6 dB to take account of the addition of the direct and ground-reflected waves at the receiver.

Fig. 2 shows the unattenuated field-strength for a range of distances measured along the surface of the Earth. In calculating $d$, the F-layer was assumed to have a virtual height of 220 km, and the height of the E-layer was assumed to vary between 100 km at vertical incidence and 90 km at very oblique incidence; these heights were derived from ray-tracing computations with a model ionosphere.[2,3]

* On short-distance paths near the magnetic equator a different orientation may sometimes give greater pick-up.

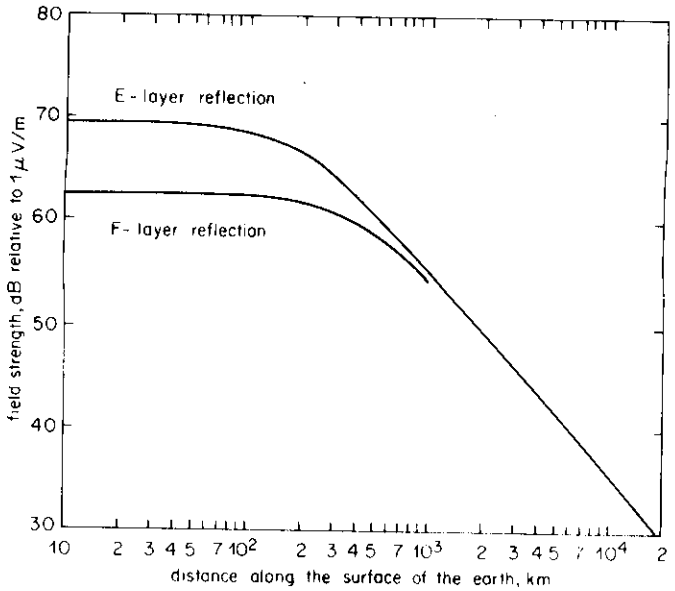


*Fig. 2 - Unattenuated field strength*

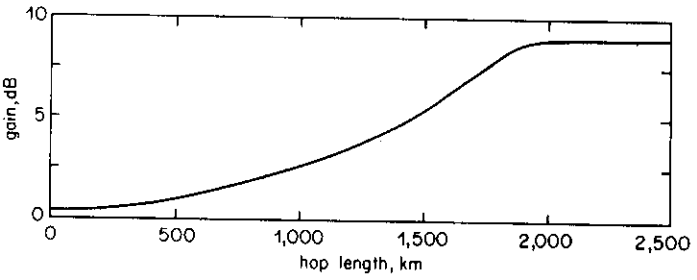


*Fig. 3 - Convergence gain*

Fig. 2 makes no allowance for convergence gain, which is discussed in the next section.

### 2.3. Convergence gain

The ionosphere behaves as a spherical mirror and causes a certain amount of focussing, thereby increasing the signal strength by an amount known as the convergence gain. This gain is greatest at very oblique incidence, where it is subject to an upper limit of about 9 dB because waves are returned from the ionosphere by refraction rather than by specular reflection. Curves of convergence gain vs radiation angle which take refraction into account have been calculated by Bradley.[4] Fig. 3 which is derived mainly from Bradley's curves, shows convergence gain for E-layer reflections as a function of hop length measured along the surface of the Earth. The convergence gain for F-layer reflections for hop lengths less than 1000 km is similar.

Although Fig. 3 was calculated for single-hop paths, it may be used for multi-hop paths with little error because ionospheric focussing on subsequent hops is approximately cancelled by defocussing at the intermediate ground reflections. It is important to note that Fig. 3 gives convergence gain as a function of hop length and not path length, and that the gain must not be included in the calculation more than once.

Since the unattenuated field strength and convergence gain are assumed to be independent of frequency, both may be combined in a single set of curves.

### 2.4. Radiation angle

An important parameter is the radiation angle, since this affects the ground loss at transmitter and receiver, the intermediate reflection loss, and, to a lesser extent, the polarisation coupling loss.

The ray-tracing computer program described in Reference 3 gives the distance at which a wave returns to Earth for a specified radiation angle. This distance depends on the virtual height of the reflecting layer and therefore varies with frequency and direction of propa-

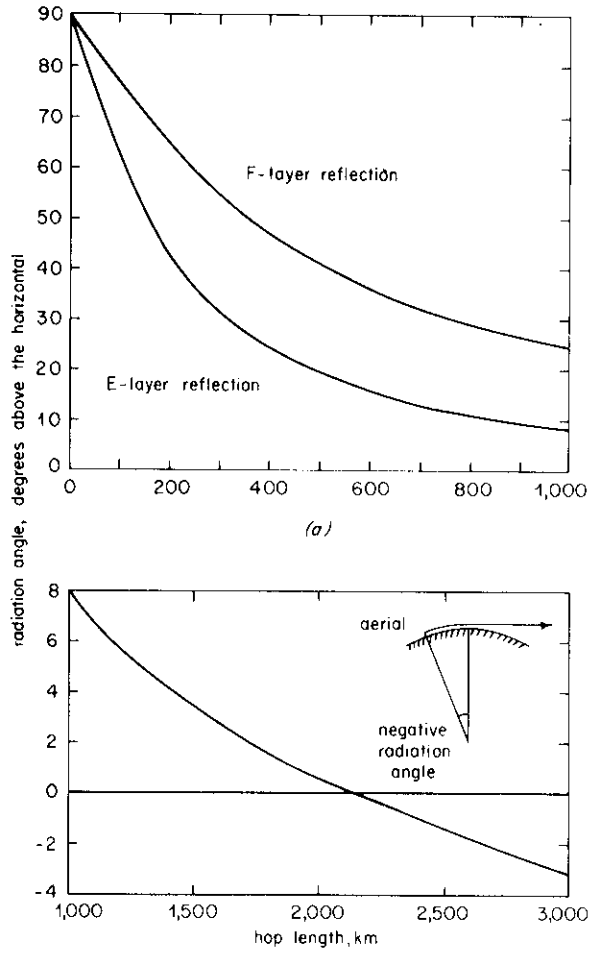


*Fig. 4 - Radiation angle*

(*a*) short distances (*b*) longer distances : E-layer reflection only

gation. An extensive series of ray-tracing computations for temperate and equatorial latitudes, for all directions of propagation and for frequencies throughout the m.f. band, has shown that the relationship between radiation angle and range is remarkably constant; a single curve for each layer therefore suffices.

Fig. 4 shows radiation-angle curves for E- and F-layer reflections, derived from the ray-tracing computations.* Fig. 4 may also be used to obtain the angle of arrival at the receiver even though it may differ slightly from the radiation angle because of ionospheric tilts and effects caused by the Earth's magnetic field; for all practical purposes the two angles may be assumed to be equal.

It will be seen that Fig. 4(*b*) has been extended to include negative radiation angles; these correspond to diffraction around the curvature of the Earth, and are defined in the inset to Fig. 4(*b*). To preserve symmetry and so avoid a discontinuity in the curve, the diffraction angles are assumed to be the same at both ends of the path, although they may in fact be unequal; this point is discussed further in the next section. In calculating the negative radiation angles shown in Fig. 4(*b*), allowance was made for atmospheric refraction, which has the effect of increasing the radius of curvature of the Earth by a factor of about 1·25 at medium frequencies.[5]

Fig. 4 may be used for multi-hop paths provided the path length is divided by the number of hops. If the hop-length exceeds 2,100 km, diffraction will occur at the intermediate Earth reflection points as well as at the terminals; such multi-hop modes are unlikely to contribute significantly to the signals received over very long paths, however, because of the high total diffraction loss.

### 2.5. Ground loss at transmitter and receiver

In calculating the unattenuated field strength shown in Fig. 2, the transmitter was assumed to radiate with a c.m.f. of 300 volts in all directions above the horizontal. Although this assumes a hypothetical reference aerial, the concept enables the actual field strength to be calculated for any practical aerial system.

In designing such a system, it is usual to assume that the ground is perfectly conducting, the effect of finite ground conductivity being taken into account subsequently. Thus if the aerial is a vertical mast or tower, the low-angle radiation which is responsible for long-distance propagation via the ionosphere will be reduced by ground loss.[6] This loss, which is small at coastal sites and greatest at inland sites, must be applied as a correction to the unattenuated field strength. A similar correction must also be applied at the receiver, since all practical receiving aerials, including loop and ferrite-rod aerials, respond mainly to the vertically-polarised components of downcoming sky-waves.

If Earth curvature were neglected the ground loss at each end of path would be given by

$$L_g = 6 - 20 \log_{10} \left| 1 + \rho_v(\alpha) \right| \quad \text{dB} \qquad (2)$$

where $\rho_v(\alpha)$ is the Fresnel plane-wave reflection coefficient for vertically-polarised plane waves incident at angle $\alpha$ to the horizontal. Since $\rho_v = -1$ when $\alpha = 0$ for all ground conductivities, ground loss would tend to infinity at grazing incidence if the Earth were flat. Diffraction around the curvature of the Earth, however, causes ground loss to have finite values at grazing and negative radiation angles.

Diffraction around an imperfectly-conducting sphere has been studied theoretically by Wait and Conda[7] and their theory is applied here to the calculation of ground loss for radiation angles less than 5°, the radius of the Earth being increased by a factor of 1·25 to allow for atmospheric refraction. The result of the calculation, for land of various conductivities and for sea, is shown in Fig. 5 together with losses for higher angles calculated from Equation (2).

The ground-loss corrections shown in Fig. 5 are valid provided the ground is level and reasonably uniform for several kilometers in the direction of propagation. This

* All the computations used for the construction of these curves were performed with the idealised electron-density profile for six hours after sunset.[2] Although slightly shorter ranges are computed for times nearer sunset, the variation of range during the night is relatively small and may be disregarded.

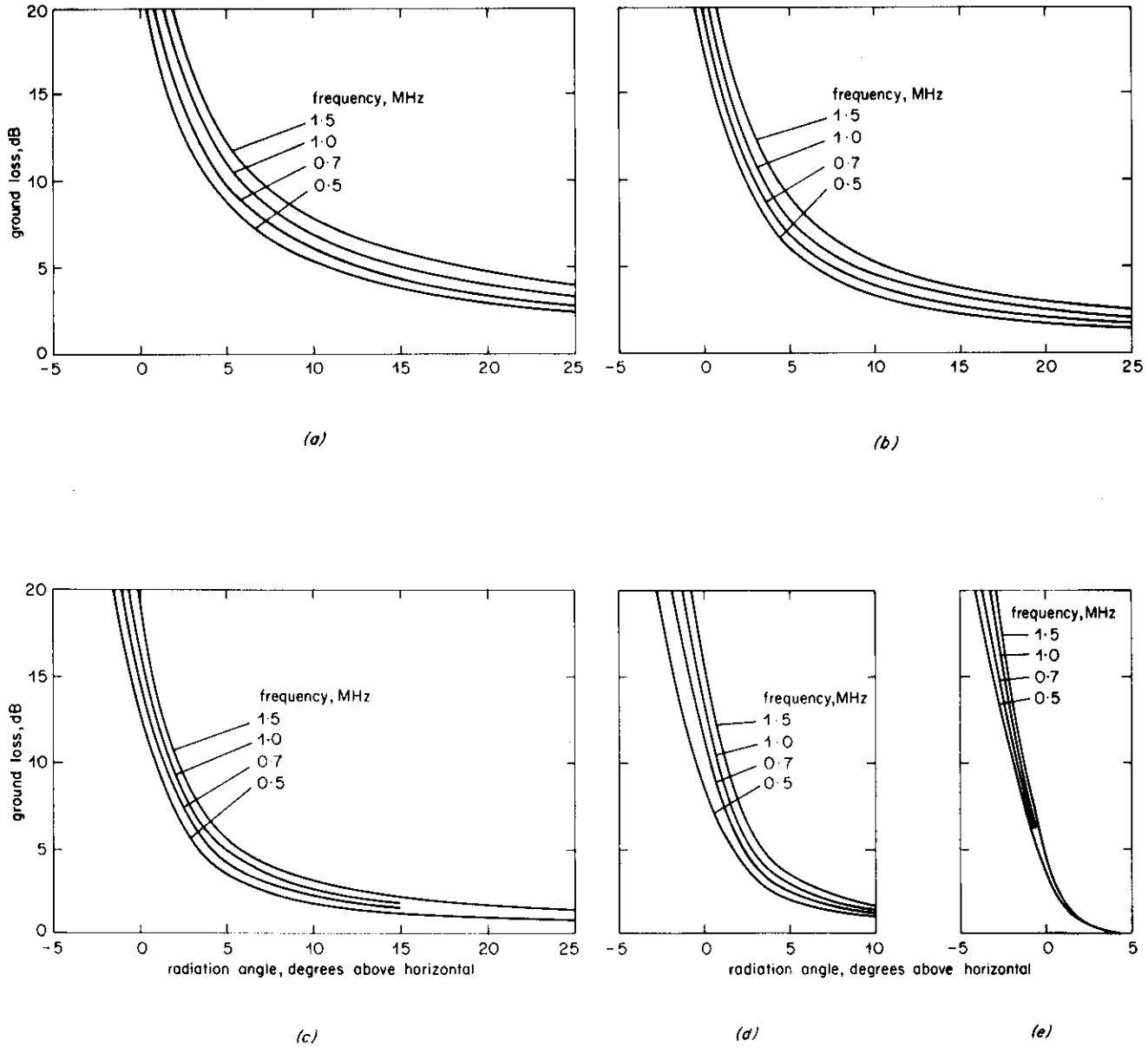


*Fig. 5 - Ground loss*

(*a*) ground conductivity 1 mS/m (*b*) ground conductivity 3 mS/m (*c*) ground conductivity 10 mS/m
(*d*) ground conductivity 30 mS/m (*e*) sea water

condition may not be satisfied if the transmitter or receiver is situated near the sea or on the edge of a sea inlet, or if the aerial is situated on sloping ground or on a hill or cliff. The ground loss which arises in such circumstances is considered in detail in Reference 6.

On single-hop paths involving diffraction around the curvature of the Earth, it is reasonable to assume that the negative radiation angles at both ends of the path are equal if the ground conductivities at the two terminals are similar. When the conductivities are very different, however, this may not be true; for example if one terminal is near the sea and the other is well inland, a greater diffraction angle might be expected at the sea terminal. Calculations assuming different combinations of diffraction angles at the terminals have shown, however, that the total ground loss on such paths does not depend critically on the way in which the total diffraction angle is shared between the two ends of the path. It may therefore be assumed to be equally divided between the two ends and given by Fig. 4(*b*) even when the conductivities are dissimilar.

### 2.6. Polarisation coupling loss at transmitter and receiver

At medium frequencies only the ordinary wave need be considered because the extraordinary wave is greatly attenuated and seldom contributes to the received signal. Waves incident on the ionosphere may be resolved into ordinary and extraordinary waves, the ratio of the power density of the ordinary wave to that of the incident wave being known as the polarisation coupling loss. It has been shown[8] that when the transmitting aerial radiates vertical polarisation, the coupling loss is given by

$$L_c = 10 \log_{10} \left( \frac{1 + M^2}{\cos^2 \psi + M^2 \sin^2 \psi} \right) \qquad (3)$$

where $M$ is the axial ratio of the ordinary-wave polarisation ellipse and $\psi$ is the angle by which its minor axis is tilted from the horizontal plane. Formulae for calculating $M$ and $\psi$ in terms of frequency, magnetic-dip latitude, direction of propagation and angle of incidence at the ionosphere are given in References 3 and 8.

When the elliptically-polarised ordinary wave which emerges from the ionosphere is received on a loop or open-wire aerial, additional coupling loss is incurred because m.f. receiving aerials respond only to the vertically-polarised components of downcoming waves. This loss is also given by Equation (3) provided $M$ and $\psi$ are the values applicable to downcoming waves.

On short-single-hop paths, curves such as those of Fig. 4 of Reference 8 may be used to determine the sum of the coupling losses at transmitter and receiver. On long paths, however, the coupling losses at transmitter and receiver must be calculated separately because the magnetic dip latitudes and directions of propagation (relative to magnetic north) at the terminals will, in general, be somewhat different. In the wave-hop method described here, coupling losses at transmitter and receiver are calculated separately for paths of all lengths.

A set of curves which give polarisation coupling losses at individual terminals are contained in Fig. 6. Although polarisation coupling loss depends to some extent on frequency and angle of incidence at the ionosphere,

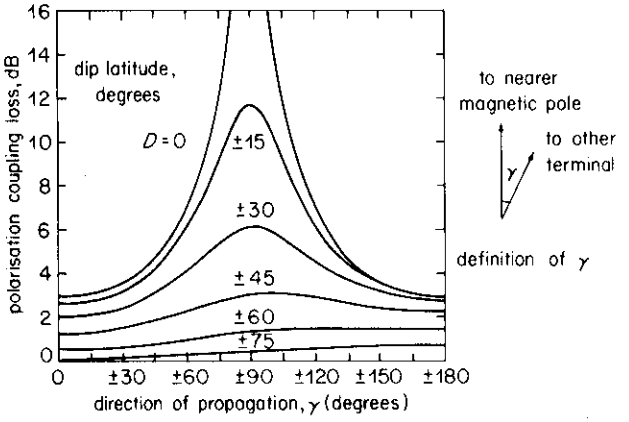


*Fig. 6 - Polarisation coupling loss at transmitter or receiver*

Fig. 6 may be used with negligible error for all frequencies in the m.f. band and for radiation angles up to 20° from the horizontal. The direction of propagation $\gamma$ is defined in the inset; on short paths the values of $\gamma$ for the two terminals tend to be complimentary. The 'nearer magnetic pole' referred to in Fig. 6 is the magnetic pole in the same hemisphere as the point where the wave enters or leaves the ionosphere.

### 2.7. Residual ionospheric absorption

At m.f., ionospheric absorption depends on time after sunset, solar activity, geomagnetism and frequency. This section considers the absorption which remains late at night during periods of low solar activity.

The Earth's magnetic field has two distinct effects on ionospheric absorption. Firstly it is responsible for the auroral zones, regions centred on the magnetic poles where absorption losses are high. Distance from the auroral zone is believed to be of considerable importance; for example, ionospheric losses in North America are known to be greater than in Europe.[9] Secondly the rate of attenuation of a wave in the ionosphere depends on the angle between its direction of propagation and the direction of the Earth's magnetic field, the rate of attenuation being least when these two directions are parallel.

These two effects in combination cause ionospheric losses on NS paths to be less than on EW paths. Long NS paths usually pass through equatorial regions, where propagation tends to be parallel to the Earth's field and auroral effects are absent. On the other hand, EW paths tend to be transverse to the Earth's field, and some EW paths (especially those across the North Atlantic) are close to the auroral zone.

The way in which ionospheric losses would vary if auroral effects were absent has been studied by means of an extensive series of ray-tracing computations, using an ionospheric model assumed to be common to all geographical areas. The model is essentially the same as that derived in Reference 2 for six hours after sunset, but all collision frequencies were halved in order to obtain reasonably good agreement between measured and predicted field strengths for Europe. The ionospheric model is therefore believed to be reasonably accurate for Europe but does not necessarily apply to other parts of the World.

The method described in Reference 3 was used for the ray-tracing computations; regional variations in the strength and direction of the Earth's magnetic field were therefore taken fully into account. A detailed study was made of propagation from hypothetical transmitters situated at Berlin and at Kaduna, Africa; Kaduna lies on the geomagnetic equator. In Europe, ionospheric losses were found to be almost independent of direction of propagation; this is to be expected because the Earth's magnetic field is almost vertical. Losses on EW paths in Europe and Africa were found to be similar; this is also to be expected because EW propagation tends to be transverse to the Earth's magnetic field at all latitudes. Furthermore, step-by-step ray-tracing computations[3] have shown that most

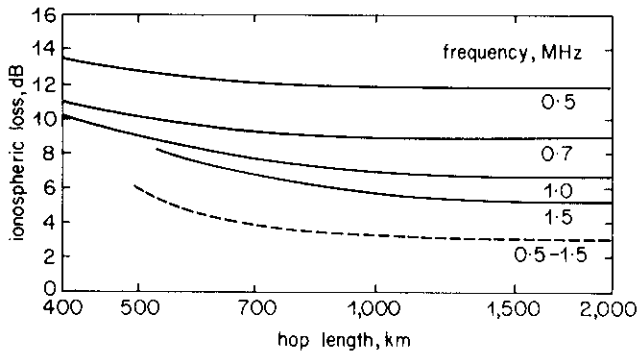


*Fig. 7 - Computed ionospheric losses*

——— East-west propagation at all latitudes ($\theta = 90^\circ$)

– – – – – – North-south propagation at magnetic equator ($\theta = 0$)

ordinary-wave attenuation occurs near the ionospheric reflection point, where EW propagation is exactly transverse and independent of the strength of the Earth's magnetic field.

Ordinary-wave losses computed for single-hop EW paths are shown by unbroken lines in Fig. 7. Although the losses decrease with increasing frequency, the reduction is less than would be expected if waves of all frequencies followed identical paths; waves of higher frequencies penetrate more deeply into the ionosphere. Fig. 7 shows that losses for low-angle modes tend to be almost independent of hop length because of the very small variation of the angle of incidence at the ionosphere.

Propagation parallel to the Earth's magnetic field was studied by computing losses on single-hop NS paths having reflection points situated at the geomagnetic equator. Although most of the computations involved reflection over Kaduna, some additional computations were made for other equatorial regions since some dependence on the strength of the Earth's magnetic field was expected. The strength of the Earth's field was, however, found to have negligible influence on the computed losses, which were also found to be almost independent of frequency. The results of the computations for equatorial NS paths are shown by the broken curve of Fig. 7.

As mentioned earlier, ionospheric loss depends on the angle $\theta$ between direction of propagation and that of the Earth's magnetic field. At the ionospheric reflection point, where most loss is incurred, the values of $\theta$ for the EW and equatorial NS paths considered here are 90° and 0 respectively. In the Appendix it is shown that the ordinary-wave loss for any other value of $\theta$ is given approximately* by

$$L_i = \frac{L_{90}\sin^2\theta + 2L_o\cos^2\theta}{1 + \cos^2\theta} \text{ dB} \qquad (4)$$

* Losses calculated from Equation (4) for paths passing over Kaduna in all possible directions relative to the NS axis have shown good agreement with losses computed for the same paths by ray-tracing.

where $L_o$ and $L_{90}$ are the losses given by Fig. 7 for $\theta = 0$ and 90° respectively. The value of $\theta$ at the ionospheric reflection point is given by

$$\cos\theta = \cos D \cos\gamma \qquad (5)$$

where $D$ is the magnetic dip latitude and $\gamma$ is the direction of propagation relative to the magnetic NS axis.

In calculating $L_i$ it is convenient to arrange Equation (4) in the form

$$L_i = L_o + (L_{90} - L_o)G \text{ dB} \qquad (6)$$

where $G = \sin^2\theta/(1 + \cos^2\theta)$

Fig. 8(*a*) is a contour chart which gives $G$ in terms of $D$ and $\gamma$.

For hop lengths greater than 1200 km Equation (6) may be further simplified to

$$L_i = 3{\cdot}0 + LG \text{ dB} \qquad (7)$$

where $L$ is the limiting value of $L_{90} - L_o$ for long hops, derived from Fig. 7 and shown in Fig. 8(*b*) as a function of frequency.

Since the losses shown in Fig. 7 were computed with an ionospheric model which may be invalid outside Europe,

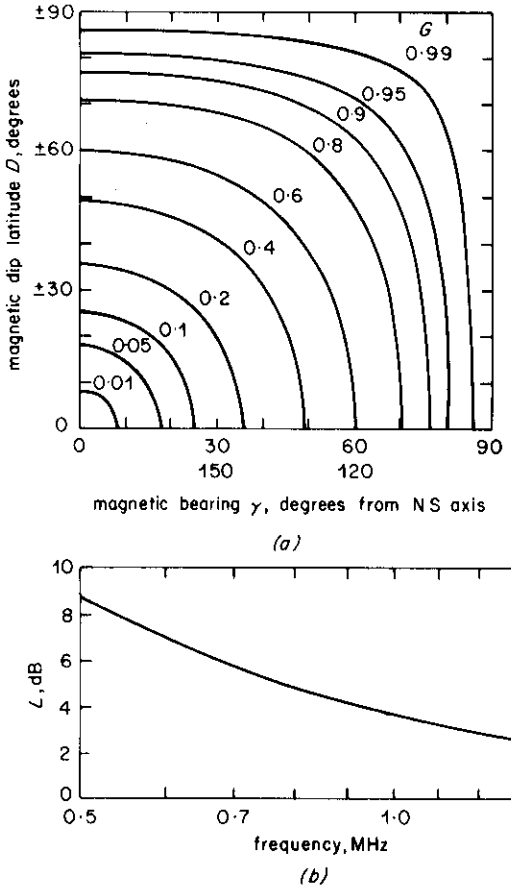


*Fig. 8 - Ionospheric loss charts*

Ionospheric loss per hop = 3·0 + $LG$ dB

(*a*) contour plot of $G$ (*b*) loss factor $L$

losses derived from Fig. 7 for other parts of the world should be treated with caution. Near the auroral zone, such losses may have to be multiplied by a factor greater than 1·0, while in tropical regions multiplication factors less than unity may be required.

### 2.8. Intermediate reflection loss

Intermediate reflection loss on multi-hop paths depends on the polarisation of the downcoming wave, the polarisation of the wave accepted by the ionosphere at the next hop, and on the ground constants. There are three situations in which the loss may be high:

1. In temperate latitudes when the downcoming wave is incident at the Brewster angle, because the ordinary wave is essentially vertically polarised
2. For East-West propagation with sea reflection at 45° dip latitude, when the ordinary wave re-enters the ionosphere as the extraordinary wave and is absorbed
3. For North-South propagation with sea reflection at the magnetic equator, when the ordinary wave is again converted into the extraordinary wave and absorbed.

Intermediate reflection loss is, in general, non-reciprocal, i.e. its value changes if the direction of propagation between two given terminals is reversed. The non-reciprocal effect is most apparant when waves are reflected from land at angles near the Brewster angle, waves propagating towards the west suffering the greater loss. Waves reflected from the sea, however, have similar losses in both directions of propagation.

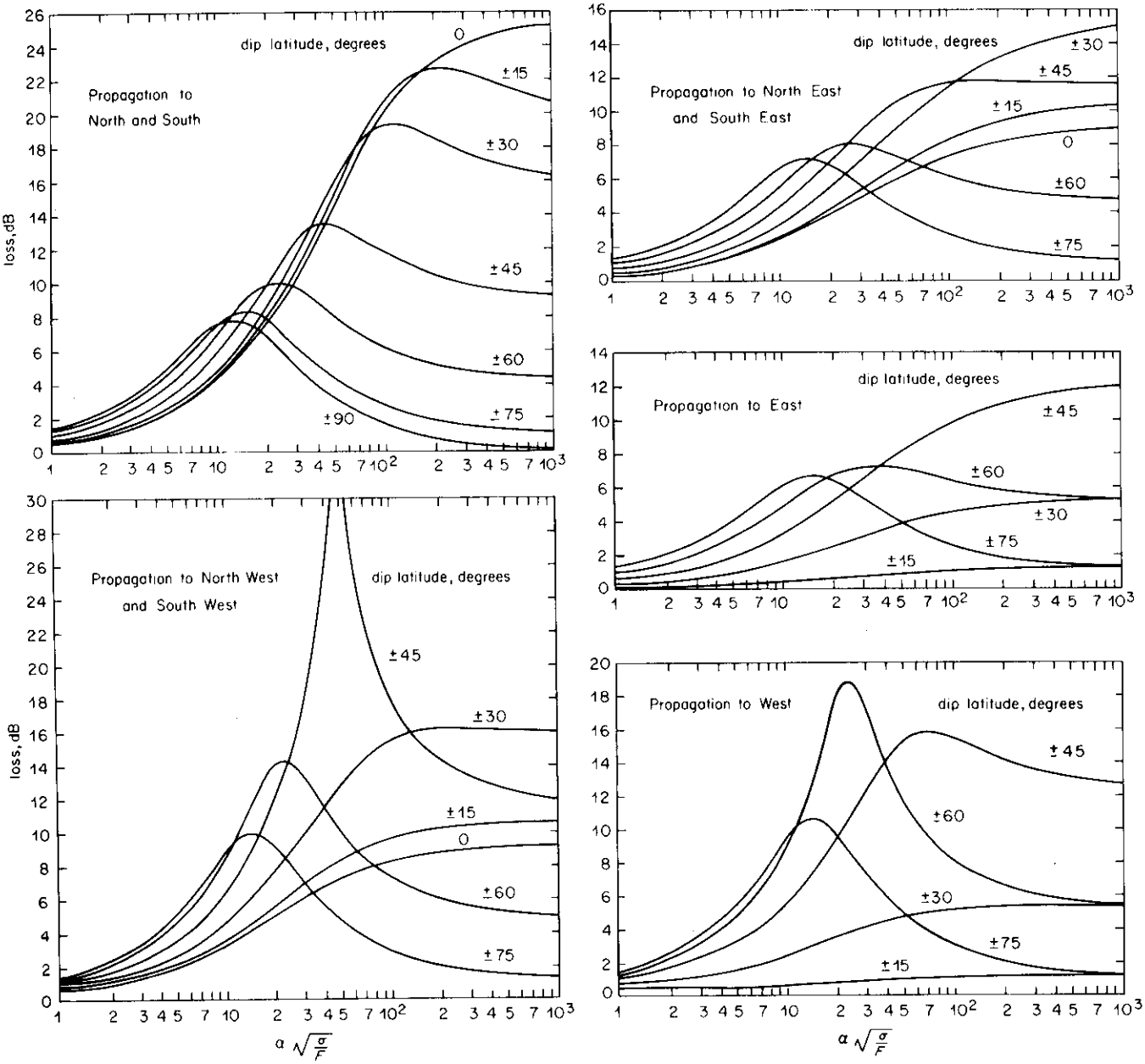


*Fig. 9 - Intermediate reflection loss*

α = angle of arrival, degrees to horizontal  σ = ground conductivity, mS/m  F = frequency, MHz  For sea water, σ ≃ 4000 mS/m

A general formula for intermediate reflection loss is derived in Reference 8 and quoted in Reference 2.* This loss is a function of a large number of variables and should, ideally, always be computed. To enable losses to be estimated from curves, however, the following simplifying assumptions have been made:

1. The dip latitude and direction of propagation at the points where the wave leaves the ionosphere, and re-enters after reflection, are the same as the value at the Earth reflection point, except on NS paths near the equator, where an allowance has been made for the change in dip latitude.

2. The frequency is approximately equal to the gyromagnetic frequency.

3. The angle of incidence at the ionosphere is 80°; this angle is approximately correct for hop lengths greater than 1000 km.

4. The reflection coefficient for horizontally-polarised radiation is −1·0.

Fig. 9 shows intermediate reflection losses, computed with these assumptions, for five directions of propagation relative to magnetic north and for a range of dip latitudes. The curves are plotted as a function of $\alpha(\sigma/F)^{\frac{1}{2}}$ where $\alpha$ is the radiation angle in degrees, $\sigma$ is the ground conductivity in mS/m and $F$ is the frequency in MHz. Because of the simplifying assumptions, Fig. 9 should not be used for values of $\alpha$ greater than 10°.

The theory described above makes no allowance for Earth curvature, which would be expected to have a significant effect when $\alpha$ is less than 2°. Although the effect of Earth curvature on intermediate reflection loss has not yet been studied, it is possible that, at grazing incidence, the loss may tend to a value of about 6 dB under all circumstances. Although greater losses would be incurred with negative radiation angles because of diffraction, multi-hop paths involving negative radiation angles are unlikely to contribute significantly to received signals.

### 2.9. Transmitting aerial correction

When two or more modes of comparable amplitude are present their combined effect must be calculated.

In calculating the strengths of individual modes the transmitter is assumed to radiate with a c.m.f. of 300 volts at all vertical angles. Before individual modes can be added, corrections must be made for the vertical radiation pattern (v.r.p.) of the transmitting aerial.

Fig. 10 shows the corrections required for vertical transmitting aerials of various heights radiating 1 kW. The corrections are similar to those given in Fig. 1 of CCIR Report 264-2, but are drawn as a function of radiation angle. No allowance has been made for imperfect ground conductivity in deriving these curves because this is taken account of in the ground loss calculation described in Section 2.5.

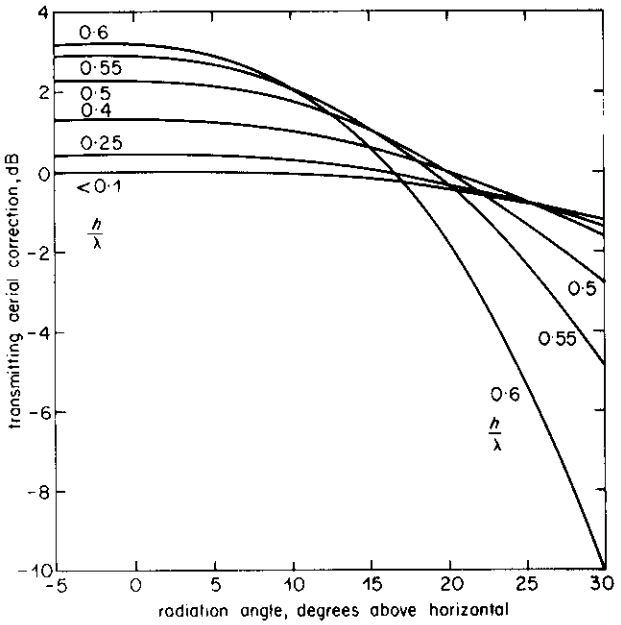


*Fig. 10 - Vertical transmitting aerial correction*
$h/\lambda$ = aerial height in wavelengths

After correction the modes are added on a power basis; Fig. 11 may be used for this operation. If more then two modes are significant, Fig. 11 may then be used to add the resultant of any two modes to a third; this process may be repeated until all the significant modes have been accounted for.

## 3. Application of the wave-hop method

To illustrate the use of the wave-hop method, its application to the Rome-Tsumeb (S.W. Africa) path is described in this section. Details of the calculation are given in Table 1.

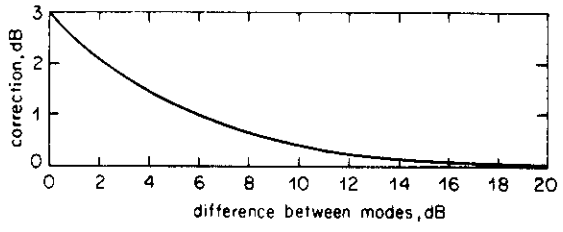


*Fig. 11 - Chart for mode addition*

* In Reference 2 the last term in the numerator of the right-hand side of Equation (15) should be $j M_2 \cos\psi_2$, not $jM_2 \sin\psi_2$.

*TABLE 1*

*Field-Strength Prediction for Rome-Tsumeb Path*

| Distance 6740 km | | | Unattenuated field strength 39·0 dBμ | | | |
|---|---|---|---|---|---|---|
| Frequency 0·845 MHz | | | Transmitting aerial 0·52λ mast radiators | | | |
| Mode | | | 4E | | | 5E |
| Hop length, km | | | 1685 | | | 1348 |
| Radiation angle | | | 2·3° | | | 4·6° |
| Convergence gain, dB | | | 6·9 | | | 4·3 |
| Transmitting aerial correction, dB | | | 2·4 | | | 2·3 |
| Field strength without losses, dBμ | | | 48·3 | | | 45·6 |
| | *D* | σ mS/m | Loss dB | *D* | σ mS/m | Loss dB |
| Ground loss at transmitter | – | 15 | 6·8 | – | 15 | 4·0 |
| Polarisation coupling loss | 50° | – | 2·3 | 51° | – | 2·3 |
| Ionospheric loss (1st hop) | 48° | – | 4·8 | 49° | – | 4·8 |
| Ground reflection loss | 32° | 8 | 3·8 | 39° | 8 | 8·0 |
| Ionospheric loss (2nd hop) | 20° | – | 3·3 | 28° | – | 3·6 |
| Ground reflection loss | 3° | 30 | 5·6 | 16° | 10 | 6·8 |
| Ionospheric loss (3rd hop) | −18° | – | 3·2 | 4° | – | 3·0 |
| Ground reflection loss | −32° | 15 | 4·8 | −15° | 15 | 7·7 |
| Ionospheric loss (4th hop) | −47° | – | 4·1 | −27° | – | 3·6 |
| Ground reflection loss | | | | −38° | 15 | 9·0 |
| Ionsopheric loss (5th hop) | | | | −50° | – | 5·0 |
| Polarisation coupling loss | −50° | – | 2·3 | −52° | – | 2·3 |
| Ground loss at receiver | – | 15 | 6·8 | – | 15 | 4·0 |
| Total loss | | | 47·8 | | | 64·1 |
| Field strength, dBμ, for 1 kW radiated | | 0·5 | | | −18·5 | |
| Predicted field strength | | | 0·6 dBμ | | | |

The path length is 6740 km and Fig. 2 indicates that the 3E, 4E and 5E modes should be considered. The radiation angle for the 3E mode is −0·3°, however, and a rough estimate shows that it is unlikely to make a significant contribution to the received signal because of the diffraction losses at the terminals and at the intermediate ground reflection points. Detailed calculations were therefore confined to the 4E and 5E modes.

In the table the sum of the unattenuated field strength, the convergence gain and the transmitting aerial correction is referred to as the 'field strength without losses', and all losses are subtracted from this figure. Before calculating individual losses it is an advantage to tabulate all the values

of dip latitude ($D$), ground conductivity ($\sigma$) and direction of propagation relative to the magnetic NS axis ($\gamma$) which are required. Values of $\gamma$ are omitted from Table 1, however, since this particular path is very close to the NS axis over its entire length.

A few points concerning the calculation for the Rome-Tsumeb path are worth mentioning. At Rome the distance to the sea in the direction of propagation is about 30 km, and the transmitter can therefore be regarded as situated on an inland site, assumed to have a conductivity of 15 mS/m. Ground conductivities at the intermediate reflection points and at the receiver were derived from the World conductivity map.[10] The polarisation coupling losses at transmitter and receiver are equal; this is unusual but it arises because the terminals are situated in opposite hemispheres at roughly the same dip latitudes.

Measurements of the Rome transmission were made at Tsumeb in 1971 by the Fernmeldetechnisches Zentralamt (FTZ) of the Deutsche Bundespost. The median field strength measured in June 1971, six hours after sunset at the northernmost ionospheric reflection point, was 37·5 dB relative to 1 $\mu$V/m (dB$\mu$). Assuming a transmitter power of 540 kW and an aerial gain, relative to that of a single 0·52$\lambda$ mast, of 2·3 dB in the direction of Tsumeb, the measured field strength would have been 7·9 dB$\mu$ if 1 kW had been radiated from a single 0·52$\lambda$ mast. The measured field strength therefore exceeds the predicted value by about 7 dB, and the discrepancy would be increased by a further 4 dB if the solar cycle correction for Europe described in Section 5.1 were taken into consideration. The discrepancy may arise because of the presence of sporadic E layers in equatorial regions; these would tend to reduce both ionospheric and intermediate reflection losses.

## 4. Comparison of measured and predicted field strengths

About 80 papers and documents which contain information about m.f. propagation at night have been studied and a detailed comparison between predicted and measured field strengths has been made. Reliable measurements made over considerable periods for 21 European paths, 26 North American paths, 22 Australian paths, 60 paths between Australia and New Zealand and 35 long-distance paths are available, together with measurements made over shorter periods for Asian and African paths, and for paths from Ascension Island. Extensive measurements have also been made in the USSR. The quantity which is usually measured is the median field strength observed during an hour, or half an hour, centred on a particular time after sunset. As these hourly (or half-hourly) medians vary considerably from night to night, the measured field strength compared with predictions is the value exceeded on 50% of the nights on which measurements were made. Measurements have been standardised to six hours after sunset where necessary and solar activity corrections have been applied to measurements made in temperate latitudes to estimate the values which would be observed at the minimum of the solar cycle.

The measured field strengths for the European paths are the values which were obtained for six hours after sunset when the measurements were subjected to the method of analysis described in Section 5.2. Those for the North American paths[11] were derived by extrapolating regression analyses of the type described in Reference 12 to zero sunspot number; 2·5 dB was then added because the measurements were made two hours after sunset. The 2·5 dB correction was also added to the Australian[13] and New Zealand[14] measurements for the same reason. The Australian measurements were not corrected for solar activity because they were made at sunspot minimum, but the EBU correction for sunspot number 80 was applied to the New Zealand measurements, full details of which were supplied to the BBC by courtesy of the Australian Post Office.

The long-distance measurements include some of the pre-war measurements from which the so-called Cairo curves were derived; they were derived from Reference 15, where 9 dB was subtracted to convert measured quasi-maximum field strengths to median values. No correction was made for solar activity. Results for the long-distance EBU paths are also given in Reference 15. The solar-activity correction was again omitted because it is uncertain what correction, if any, is required for long-distance paths.

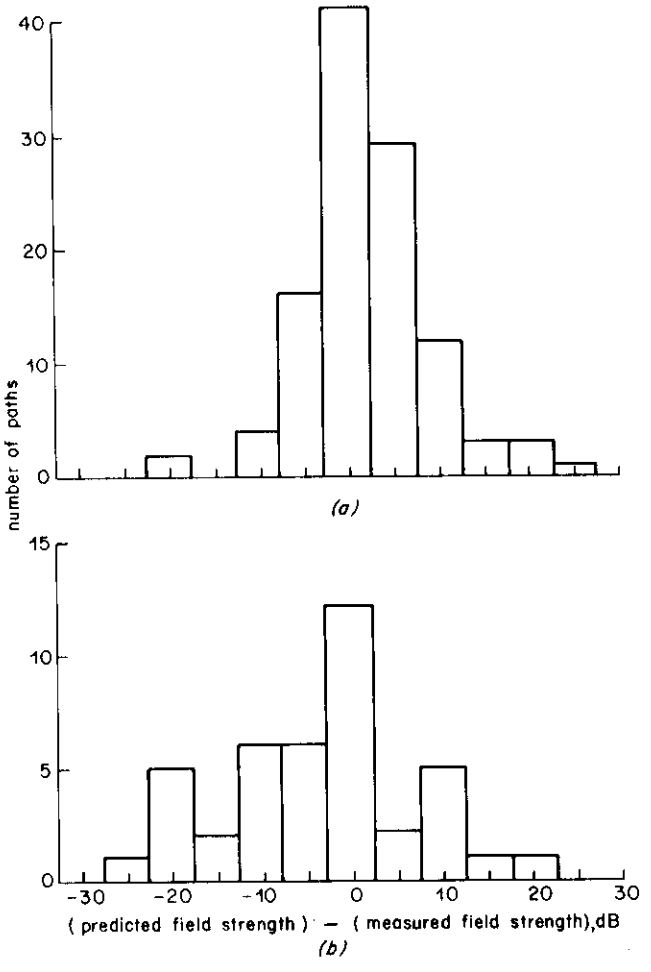


*Fig. 12 - Distribution of differences between predicted and measured field strengths*

(*a*) Paths shorter than 3000 km (*b*) Paths longer then 3000 km

Fig. 12 shows histograms of the difference between 152 predicted and measured field strengths. On paths shorter than 3000 km, 84% of the differences are less than 10 dB and on longer paths 66% of the differences come within this range. Some of the larger discrepancies may be caused by uncertainties about effective ground conductivities at transmitting and receiving sites, and at intermediate ground reflection points.

## 5. Solar-cycle, diurnal and random variations

The wave-hop method described in Section 3 predicts the median field strength six hours after sunset when solar activity is least. The quasi-maximum field strength, or the field strength at some other time of night or point in the solar cycle, may be estimated from the predicted value by means of corrections discussed in this section.

### 5.1. Solar-cycle variation

Solar activity increases ionospheric absorption loss at m.f. An analysis of measurements made in Europe[12] has shown that, as a consequence, field strengths are reduced by $Rd \times 10^{-5}$ dB, where $R$ is the sunspot number and $d$ is the path length in km. Somewhat greater field-strength variations are observed in North America[16] and Australia[17], presumably because they are close to the auroral zones. Measurements made on 26 North American paths[11] have been analysed by the method described in Reference 12 and the results show that the solar-cycle variation is approximately double that in Europe.

In general it would seem that field strengths estimated for minimum solar activity by the method described in Section 2 should be reduced by $KRd$ dB, where $K$ is a factor which may prove to be a function of distance from the auroral zones. In Europe, for example, $K$ is equal to $10^{-5}$ and in North America it is about twice this value.

### 5.2. Diurnal variation

The prediction method described in Section 3 estimates the field strength six hours after sunset. It is well-known that m.f. sky-wave field strengths are lower nearer to sunset, and at sunrise.

In order to study the diurnal variation, median field strengths measured by the EBU during half-hour periods throughout the night on about 20 European paths were classified by a computer according to the time after sunset, or before sunrise, at which the measurements were made. The EBU correction for solar activity was applied to each individual measurement, and the computer then found the field strengths exceeded for 50% of the time during consecutive half-hour periods after sunset or before sunrise. The diurnal variations obtained on all paths were found to be similar to the average variation shown in Fig. 13. Similar variations have been observed in Australia[13] and India.[18] Fig. 13 also agrees well with variations observed on very long paths, provided the time reference is local time at the hop which controls the onset of night-time propagation, or the commencement of day-time propagation.

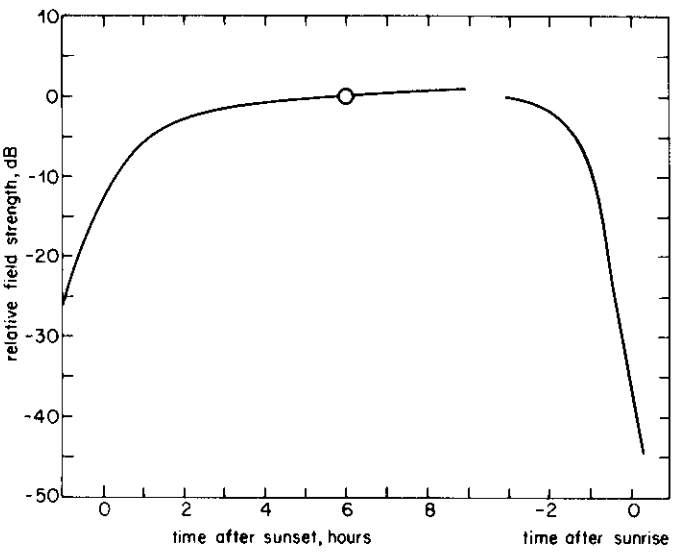


*Fig. 13 - Diurnal variation*

The reference times are the times of sunset and sunrise at sea level

Fig. 13 may be used provisionally to derive field strengths for any time during the night from predictions for six hours after sunset or from measurements made at that time. Detailed study of the results of the computer analysis may reveal some dependence of the diurnal variation on both frequency and time of year.

### 5.3. Random variation

Medium-frequency ionospheric signals fluctuate because the ionosphere is turbulant. When a single E-layer mode predominates the fading rate is slow,* but when two or more modes of comparable amplitude are present the fading rate is much more rapid.

Considerable variation in the median field strength measured during one hour is observed from night to night because of changing ionospheric conditions. The statistic which is usually quoted is the field strength which is exceeded by the hourly median on 50% of the nights of the year at a stated time after sunset. This is the quantity which is predicted by the wave-hop method described in Section 2.

A knowledge of the amount by which this field strength is exceeded for shorter periods is essential. Sufficient information appears to be available for reliable estimates to be obtained, but this aspect has not yet been studied in detail.

## 6. Propagation to short distances

The wave-hop method described in Section 2 is intended for distances greater than 500 km. It cannot be used for shorter distances in its present form because high radiation

* The number of deep fades per hour is about ten times the frequency in MHz.

angles are beyond the range of validity of many of the curves.

Experience with anti-fading mast radiators suggests that the reflection coefficient of the ionosphere in Europe rises a maximum value of about −10 dB late at night, at all frequencies in the m.f. band. Thus the maximum field strength which is likely to be observed in Europe may be estimated from the unattenuated field strength given in Fig. 2 by subtracting 10 dB, the appropriate reflecting layer or layers being determined by reference to Fig. 1(*a*). Actual field strengths may sometimes be much lower than values predicted in this way, especially when reflected waves are about to penetrate the E-layer.

Of the 10 dB of residual attenuation, 4 to 6 dB is accounted for by polarisation coupling loss and the remainder is due to ionospheric absorption. In other temperate latitudes the polarisation coupling loss will be similar but the ionospheric absorption may be significantly different. In tropical latitudes, polarisation coupling loss will be low on North South paths and high on East West paths unless transmissions are radiated from horizontal aerials, discussed further in the next section.

## 7. Horizontal transmitting aerials

In the prediction method described in Section 2 the transmitting aerial is assumed to be vertical. Horizontal aerials are sometimes used for short-distance sky-wave broadcasting, however, and their use calls for some modifications to the prediction method which are discussed in this section.

The principal factors which must be taken into consideration are the change in polarisation coupling loss and the effect of finite ground conductivity. Once the wave has entered the ionosphere its propagation is independent of the transmitter which excited it, and no further modifications to the preferred method are required.

In general, horizontal aerials radiate elliptical polarisation and the calculation of polarisation coupling loss is complicated. The calculation is, however, relatively simple in the following situations:

1. at the high angles corresponding to the service area, where the radiation is essentially plane polarised. In European and other temperate latitudes the total coupling loss for both ends of the path will be 4 to 6 dB, as with vertical transmitting aerials. In tropical latitudes the polarisation coupling loss at the transmitting end of the path will be low provided the axes of the horizontal dipoles lie in a magnetic North South direction; if they lie East West, however, the coupling loss will be very high.

2. in the 'broadside' directions, where the radiation is horizontally polarised. For low-angle radiation, the polarisation coupling loss at the transmitting end of the path may be derived by adding 1 dB to the values shown in Fig. 4 of Reference 19.

3. in the 'end-on' directions, where the radiation is vertically polarised and the coupling loss is exactly the same as that calculated for vertical aerials, described in Section 2.6.

At low angles the effect of finite ground conductivity and Earth curvature must be taken into consideration. In the 'end-on' directions, finite ground conductivity increases, rather than decreases, the strength of low angle radiation compared with that which would be observed if the ground were perfectly conducting.[19] The effect of Earth curvature has not yet been studied.

Since the prediction method is based on a semi-isotropic transmitting aerial whose c.m.f. is 300 volts, curves similar to those of Fig. 10 must be used to correct for the v.r.p.s of horizontal transmitting aerials. Beyond the service area, multi-hop high-angle F-layer modes may predominate because horizontal aerials radiate more strongly at high angles.

## 8. Discussion

The wave-hop method relies on the calculation of as many of the factors which control m.f. ionospheric propagation as possible. Errors are therefore mainly caused by uncertainty about those factors which cannot be calculated but must be derived from measurement. The principal source of error is lack of knowledge about the variation of ionsopheric absorption with latitude and with solar activity. Uncertainty about ground conductivities also leads to errors, especially when low-angle modes are involved.

To obtain more precise information about ionospheric absorption, a detailed comparison of predicted and measured field strengths on paths of about 1000 km needs to be undertaken. If this can be done for as many regions as possible, a world-wide picture of the variation of absorption should result. It may be possible to incorporate this variation in the prediction method, possibly as an ionospheric-loss multiplication factor which depends on geographical location.

Application of the wave-hop method tends to be laborious and time-consuming, especially when long-distance paths are concerned. To facilitate its use it may be desirable to translate it into a computer program, especially as some factors, such as intermediate ground reflection loss, are more conveniently obtained by computation. A disadvantage, however, is that a world map of ground conductivity would have to be stored in the computer, together with less detailed information about the strength and direction of the Earth's magnetic field. An alternative would be to use the method to calculate propagation curves for typical conditions; this approach may be quite satisfactory for distances up to about 3000 km.

## 9. References

1. CCIR Report 265-2, Section 2.

2. KNIGHT, P. M.F. propagation: the behaviour of the normal ionosphere during the night and at sunrise. BBC Research Department Report 1971/22.

3. OLVER, A.D., LYNER, A.G. *and* KNIGHT, P. 1971. A computer programme for calculating sky-wave field strengths at medium frequencies. *EBU Rev.*, 1971, **125A**, pp. 18 – 27.

4. BRADLEY, P.A. 1970. Focussing of radio waves reflected from the ionosphere at low angles of elevation. *Electron. Letters*, 1970, **6**, 15, pp. 457 – 458.

5. ROTHERHAM, S. 1970. Ground-wave propagation at medium and low frequencies. *Electron. Letters*, 1970, **6**, 25, pp. 794 – 795.

6. KNIGHT, P. *and* THODAY, R.D.C. 1969. Influence of the ground near transmitting and receiving aerials on the strength of medium-frequency sky waves. *Proc. IEE*, 1969, **116**, 6, pp. 911 – 919.

7. WAIT, J.R. *and* CONDA, A.M. 1958. Pattern of an antenna on a curved lossy surface. *IRE Trans. Antennas and Propag.*, 1958, **AP–6**, 4, pp. 348 – 359.

8. PHILLIPS, G.J. *and* KNIGHT, P. 1964. Effects of polarisation on a medium-frequency sky-wave service, including the case of multi hop paths. *Proc. IEE*, 1965, **112**, 1, pp. 31 – 39.

9. BARGHAUSEN, A.F. 1966. Medium-frequency sky wave propagation in middle and low latitudes. *IEEE Trans. Broadcasting*, 1966, **BC–12**, 1, pp. 1 – 14.

10. ALBRECHT, H.J. 1970. Geographical distribution of electrical ground parameters and effects on navigational systems. AGARD Conference Proceedings No. 33, pp. 337 – 347 (1970).

11. Long term sky wave field strength measurements in the 550 – 1600 kHz frequency band. FCC Report No. R-7103, 1971.

12. DREWERY, J.O. *and* KNIGHT, P. Variation of medium-frequency sky-wave field strength with solar activity in Europe. BBC Research Department Report 1971/11.

13. Medium frequency sky-wave field strength predictions for Australia. CCIR Doc. VI/205, 23 June 1966.

14. Sky-wave propagation at frequencies below 1500 kHz. CCIR Doc. VI/5, 26 August 1969.

15. Long-distance propagation in Band 6 (MF). CCIR Doc. 6/97, 6 April 1972.

16. BARGHAUSEN, A.F. *and* LILLIE, D.A. 1965. Some evidence of the influence of long-term magnetic activity on medium frequency sky wave propagation. *Proc. IEEE*, 1965, **53**, 12, pp. 2115 – 6.

17. DIXON, J.M. 1960. Some medium frequency sky-wave measurements. *Proc. Instn. Radio Engrs., Australia*, 1960, **21**, 6, pp. 407 – 409.

18. Medium frequency sky wave service (All India Radio). ABU Doc. E/21, Engineering committee meeting, Shiraz, Iran, October 1972.

19. KNIGHT, P. M.F. propagation: the reduction of interference by the use of horizontal-dipole transmitting aerials. BBC Research Department Report No. 1972/21.

20. KNIGHT, P. 1972. Radio-wave propagation in the lower ionosphere during the night, at medium and low frequencies. Ph.D. Thesis, London University, January 1972.

21. RATCLIFFE, J.A. 1959. The magneto-ionic theory. Cambridge University Press, 1959.

22. KNIGHT, P. The polarization of waves reflected from the ionosphere. BBC Research Department Report No. 1969/31.

## 10. Appendix

### Ionospheric attenuation of the ordinary wave

It has been shown[20] that the imaginary part $\chi$ of the complex refractive index of a wave of any polarisation traversing the lower ionosphere is given by

$$\chi = \frac{XZ}{4(1+RR^*)}\left[\frac{2\sin^2\theta}{1+Z^2} + \frac{(\cos\theta + jR)(\cos\theta - jR^*)}{(1+Y)^2+Z^2} + \right.$$

$$\left. + \frac{(\cos\theta - jR)(\cos\theta + jR^*)}{(1-Y)^2+Z^2}\right] \qquad (8)$$

where the asterisk denotes the complex conjugate and the symbols have the usual meanings ascribed to them in the magneto-ionic theory.[21] The rate of attenuation of the wave is described by the equation

$$\frac{dP}{dz} = -2kP\chi \qquad (9)$$

where $P$ is the power density of the wave, $z$ is distance in the direction of propagation, $k = 2\pi/\lambda$ and $\lambda$ is the wavelength.

The polarisation of the ordinary wave is given approximately by

$$R = -j\cos\theta \qquad (10)$$

if (1) the frequency is close to the gyromagnetic frequency (as at m.f.) and (2) electron-molecule collisions have a negligible effect on polarisation (justified elsewhere[22]).

Equation (10) is exact when $\theta = 0$ and 90° and it may be shown that Equation (8) then simplifies to

$$\chi_o = \frac{XZ}{2[(1+Y)^2+Z^2]} \quad \text{when } \theta = 0 \qquad (11)$$

$$\chi_{90} = \frac{XZ}{2(1+Z^2)} \quad \text{when } \theta = 90° \qquad (12)$$

If Equations (10), (11) and (12) are substituted in Equation (8) it may be shown that

$$\chi = \frac{\chi_{90}\sin^2\theta + 2\chi_o\cos^2\theta}{1+\cos^2\theta} \qquad (13)$$

Equation (13) applies to every point on the path. Since the variation of $\theta$ along the path is relatively small in the region where most ionospheric absorption takes place, $\theta$ may be assumed to be constant with little error. If Equation (13) is substituted in Equation (9) and then integrated, it may be shown that the total ionospheric loss for any given value of $\theta$ is given by

$$L_i = \frac{L_{90}\sin^2\theta + 2L_o\cos^2\theta}{1+\cos^2\theta} \quad \text{dB} \qquad (14)$$

where $L_o$ and $L_{90}$ are the ionospheric losses in dBs when $\theta = 0$ and 90° respectively.

SMW/JUC



Printed by BBC Research Department, Kingswood Warren, Tadworth, Surrey